Article

pubs.acs.org/Biomac

Block and Random Copolymers Bearing Cholic Acid and Oligo(ethylene glycol) Pendant Groups: Aggregation, Thermosensitivity, and Drug Loading

Yu Shao,[†] Yong-Guang Jia,[†] Changying Shi,[‡] Juntao Luo,[‡] and X. X. Zhu*,[†]

[†]Département de Chimie, Université de Montréal, C.P. 6128, Succ. Centre-ville, Montréal, Quebec H3C 3J7, Canada

[‡]Department of Pharmacology, State University of New York Upstate Medical University, Syracuse, New York 13210, United States

Supporting Information

ABSTRACT: A series of block and random copolymers consisting of oligo(ethylene glycol) and cholic acid pendant groups were synthesized via ring-opening metathesis polymerization of their norbornene derivatives. These block and random copolymers were designed to have similar molecular weights and comonomer ratios; both types of copolymers showed thermosensitivity in aqueous solutions with similar cloud points. The copolymers self-assembled into micelles in water as shown by dynamic light scattering and transmission electron microscopy. The hydrodynamic diameter of the micelles formed by the block copolymer is much larger and exhibited a broad and gradual shrinkage from 20 to 54 °C below its cloud point, while the micelles formed by the random copolymers are smaller in size but exhibited some swelling in the same temperature range. Based on *in vitro* drug release studies, 78% and 24% paclitaxel (PTX) were released in 24 h from micelles self-assembled by the block and random copolymers, respectively. PTX-loaded micelles formed by the block and random copolymers exhibited apparent antitumor efficacy toward the ovarian cancer cells with a particularly low half-maximal inhibitory concentration (IC_{50}) of 27.4 and 40.2 ng/mL, respectively. Cholic acid-based micelles show promise as a versatile and potent platform for cancer chemotherapy.

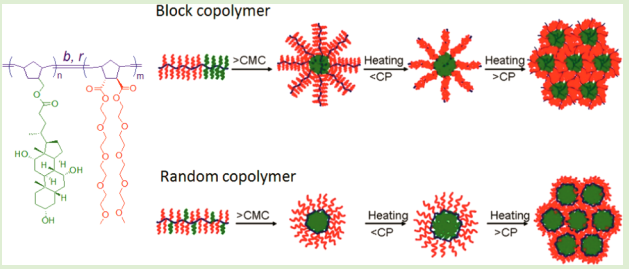

INTRODUCTION

Amphiphilic polymers capable of self-assembly have attracted much research interest in many fields, including medicine and biology.[1] In particular, self-assembled polymeric micelles have been tested as drug carriers for hydrophobic anticancer drugs.[2,3] The advent of "living polymerization" methods[4,5] facilitated the synthesis of the well-defined polymers with desired structures. More recently, living ring-opening metathesis polymerization (ROMP), a variation of the olefin metathesis reaction, has emerged as a powerful method for synthesizing polymers with tunable sizes, shapes, and functions. The technique has found tremendous utility in preparing materials with interesting biological, electronic, and mechanical properties.[6,7] Furthermore, the polymer structure can be fine-tuned by modulating the overall molar mass, amphiphilicity, and choice of blocks. In aqueous media, the formation of polymeric micelles may help encapsulate hydrophobic therapeutic compounds.[8] Most studies on polymeric micelles have focused on amphiphilic block copolymers.[9] In contrast, random copolymers have not been extensively studied due to their ill-defined properties[10] and structures.[11]

Thermoresponsive polymeric micelles based on poly(*N*-isopropylacrylamide) (PNIPAM) were studied as drug carriers.[12−16] Zhuo and co-workers reported that micelles formed by poly(*N*-isopropylacrylamide-*b*-methyl methacrylate) (PNIPAM-*b*-PMMA) showed a thermoresponsive switching behavior for the release of prednisone acetate.[14] Thermoresponsive polymers composed of oligo(ethylene glycol) are more promising compared with their PNIPAM-based polymers in such applications since they are neutral, nontoxic, and nonimmunogenic.[17,18] Lutz et al. developed oligo(ethylene glycol) methacrylate-based thermosensitive polymers with a tunable could point (CP).[19,20] These oligo(ethylene glycol)-based copolymers were conjugated with trypsin and exhibited a higher enzymatic activity than unmodified trypsin.[20] Slugovc and co-workers studied the polymerization behavior of norbornene derivatives with oligo(ethylene glycol) monomethyl ether moieties with Grubbs catalyst. Monomers bearing short oligo(ethylene glycol)monomethyl ether moieties allowed for controlled polymerization. These polymers all showed satisfactory water solubility and CPs.[21] Cholic acid, an important natural compound existing in large quantities in animals, is an ideal building block for biomimetic systems due to the rigidity of its steroid ring, amphiphilic property, and the possibility of functionalization.[22,23] It is thus of interest to design polymers consisting of oligo(ethylene glycol) and cholic acid with thermoresponsive and self-assembly properties. Polymers bearing a dendritic cluster of cholic acids and

Received: February 12, 2014
Revised: March 31, 2014
Published: April 11, 2014

   dx.doi.org/10.1021/bm5002262 | *Biomacromolecules* 2014, 15, 1837−1844

poly(ethylene glycol) (PEG) were tested as carriers for anticancer drugs. They were found to form nanocarriers with high drug-loading capacity and excellent stability *in vitro* and *in vivo*.[24,25]

Our group has developed functional responsive polymers based on (meth)acrylic derivatives of bile acids.[26−30] In this work, we prepared new monomers of PEG and cholic acid based on norbornene derivatives and made block and random copolymers via ROMP method. The self-assembly and thermoresponsive properties of these copolymers were studied. *In vitro* drug release and cytotoxicity of paclitaxel-loaded micelles from these copolymers were also investigated.

EXPERIMENTAL SECTION

Materials. Paclitaxel (PTX) was purchased from AK Scientific Inc. (Mountain View, CA). Dialysis membrane with 3500 MWCO was purchased from Spectrum Laboratories, Inc. Cholic acid, 5-norbornene-2-methanol (mixture of *endo* and *exo*, 98%), 5-norbornene-2-endo,3-exo-dicarboxylic acid, tetraethylene glycol monomethyl ether, 4-(dimethylamino)pyridine (DMAP), ethyl vinyl ether, 3-bromopyridine, 1-ethyl-3-(3-(dimethylamino)propyl)carbodiimide hydrochloride (EDC·HCl), pyrene, (1,3-bis(2,4,6-trimethylphenyl)-2-imidazolidinylidene)-dichloro(phenylmethylene)-(tricyclohexylphosphine)ruthenium (second generation Grubbs' catalyst), and CellTiter 96 AQ_{ueous} MTS Reagent Powder were purchased from Promega (Madison, WI, USA). Milli-Q water was used throughout the experiments. Dichloromethane (DCM) was dried using a solvent purification system from Glass Contour. Hexane, methanol, and ethyl acetate were used without further purification. Third generation Grubbs' catalyst was synthesized from second generation Grubbs' catalyst as described previously.[31] The purities of the monomers used in this study were confirmed by NMR and thin-layer chromatography (TLC) (>95%).

Characterization. ^{1}H and ^{13}C NMR spectra in $CDCl_3$ or D_2O were recorded on a Bruker AV400 spectrometer operating at 400 MHz for ^{1}H and 100 MHz for ^{13}C. Fluorescence spectra were recorded on an FLS-900 (Edinburgh Instruments, UK) fluorescence spectrophotometer equipped with Xe-900 lamp. The slit widths of excitation and emission were 5 and 0.2 nm, respectively. The amounts of pyrene were chosen to reach a pyrene saturated concentration in the final suspension of 6×10^{-7} M. The samples were equilibrated by shaking overnight at 20 °C. Excitation spectra were recorded in the range of 300−360 nm with a fixed emission at 390 nm. The critical micelle concentration (CMC) is taken as the intersection of the tangent to the curve at the inflection with the horizontal tangent through the points at low polymer concentrations.

Size exclusion chromatography (SEC) was performed on a Breeze system from Waters equipped with a 717 plus autosampler, a 1525 Binary HPLC pump, and a 2410 refractive index detector using three consecutive Waters columns (Phenomenex, 5 μm, 300 mm × 7.8 mm; Styragel HR4, 5 μm, 300 mm × 7.8 mm; Styragel HR6, 5 μm, 300 × 3.8 mm). DMF containing 0.1 M LiBr was filtered using 0.2 μm nylon Millipore filters for eluent solvent (flow rate: 1 mL/min). Poly(methyl methacrylate) standards (2500−608 000 g/mol) were used for calibration.

Transmission electron microscopy (TEM) was done on a FEI Tecnai 12 TEM equipped with a Gatan 792 Bioscan 1k × 1k wide-angle multiscan CCD camera with an accelerating voltage of 120 kV. The samples were prepared by placing a drop of polymer solution (0.1 g/L in water) on 300 mesh carbon-coated copper grids (Carbon Type B with Formvar, from Ted Pella, Inc.). The solution was frozen in liquid nitrogen, followed by the removal of water through freeze−drying.

The cloud point (CP) of the polymers was determined by the optical transmittance on a Cary 300 Bio UV−vis spectrophotometer equipped with a temperature-controlled sample holder. The absorbance was accessed with continuous heating or cooling rate of 0.5 °C/min with different concentrations over various temperature ranges. The CP was determined from the middle point between the onset and the offset of the transmittance curve as a function of temperature.

Dynamic light scattering (DLS) measurements were performed on a Malvern Zetasizer NanoZS instrument (Malvern CGS-2 apparatus) equipped with a He−Ne Laser at a wavelength of 633 nm and a scattering angle of 173°. The temperature was controlled in the range of 20−70 °C. Intensity-average hydrodynamic diameters of the dispersions were obtained by DLS using non-negative least-squares (NNLS) algorithm. The suspensions were prepared with the concentration of 2.0 g/L and filtered through 0.2 μm Millipore filters to remove dust. The sample was heated at 2 °C intervals within 300 s equilibration time.

The static light scattering (SLS) experiments were conducted on a CGS-3 compact goniometer (ALV GmbH) equipped with an ALV-5000 multi τ digital real time correlator at selected temperatures using a Science/Electronics temperature controller. The laser wavelength was 632 nm. The angular range was between 30° and 150° with increments of 10°. The polymer solutions (2 g/L) were filtered in an atmosphere of filtered air through a 0.2 μm filter (Millipore) directly into precleaned 10 mm tubes (Wilmad Glass Co.). The SLS experiments were conducted at fixed temperatures (25 and 50 °C). The samples were heated from 25 °C to the desired temperature with a heating rate of 0.5 °C/min and then measured after the stabilization of the temperature. The standard (toluene) and solvent (water) used to calculate the Rayleigh ratio, $R_{vv}(q)$, were also measured at each temperature. The weight-average molar mass (M_w) of the micelles at different temperatures were measured according to the previous literature.[32]

Monomer Synthesis. Cholic acid-based norbornene monomer (NCA) was prepared as described previously.[33] 5-Norbornene-2-endo,3-exo-dicarboxylic acid bis(tetraethylene glycol monomethyl ether) ester (NOEG) was synthesized according to the literature with minor modifications.[34,35] 5-Norbornene-2-endo,3-exo-dicarboxylic acid (3.20 g, 17.57 mmol) and excess thionyl chloride (25 mL, 352.19 mmol) were added into a dry round-bottom flask. 5-Norbornene-2-endo,3-exo-dicarboxylic acid chloride was obtained by refluxing the mixture above for 4 h at 90 °C and subsequently removing excess of thionyl chloride under reduced pressure, and then dissolved in dry DCM (35 mL) without further purification. Tetra(ethylene glycol) monomethyl ether (9.13 g, 43.91 mmol) and 4-dimethylaminopyridine (DMAP, 0.215 g, 1.76 mmol) were added. The reaction mixture was cooled with an ice bath, and pyridine (3.5 mL, 43.45 mmol) was added dropwise. The mixture was stirred for 24 h at room temperature ($CHCl_3$:MeOH = 20:1; detection: $KMnO_4$ solution). The white precipitate was removed by filtration and then the organic layer was washed with 5% HCl solution and dried with Na_2SO_4. The crude product was purified by column chromatography (silica; $CHCl_3$:MeOH = 100:1). Yield: 76%. FT-IR (ATR mode): ν (cm^{-1}), 2871 (CH_2), 1727 (C═O), 1108 (C−O). ^{1}H NMR ($CDCl_3$, 400 MHz): δ (ppm) = 6.28 (dd, J^1 = 3.2 Hz, J^2 = 5.6, 1H), 6.08 (dd, J^1 = 2.8 Hz, J^2 = 5.6, 1H), 4.24 (m, 4H), 3.73−3.55 (m, 28H), 3.44 (t, J = 4 Hz, 1H), 3.39 (s, 6H), 3.3 (br s, 1H), 3.15 (br s, 1H), 1.82 (s, 1H), 1.62 (d, J = 8.8 Hz, 1H), 1.45 (dd, J^1 = 1.6 Hz, J^2 = 8.8, 1H). ^{13}C NMR (100 MHz, $CDCl_3$): δ (ppm) = 174.3, 173.1, 137.5, 135.1, 71.9, 70.6, 70.5, 69.1, 63.9, 63.6, 59.0, 47.9, 47.7, 47.2, 47.1, 45.8. HRMS (ESI Pos): found for $C_{27}H_{46}O_{12}$ $[M + 1]^+$: 563.307 m/z, calculated 563.306 m/z.

Polymerization. All polymerizations were performed under argon atmosphere. Solvents were degassed by a freeze−pump−thaw procedure. The block copolymers were prepared by the sequential addition of the respective monomers. The general synthetic procedure of block copolymer $PNOEG_{34}$-*b*-$PNCA_8$ is described below. NOEG (214 mg, 0.38 mmol) in 1 mL DCM was added into an argon-flushed Schlenk tube equipped with a magnetic stir bar. Third generation Grubbs' catalyst (10.0 mg, 11.3×10^{-3} mmol) in 0.1 mL DCM was added to the monomer solution under stirring. The polymerization was carried out at room temperature for 3 h until all NOEG was consumed. NCA (48.0 mg, 0.09 mmol) in 0.25 mL DCM was added to the above mixture and stirred for 3 h at room temperature until all

Scheme 1. Synthesis of Block Copolymers via ROMP

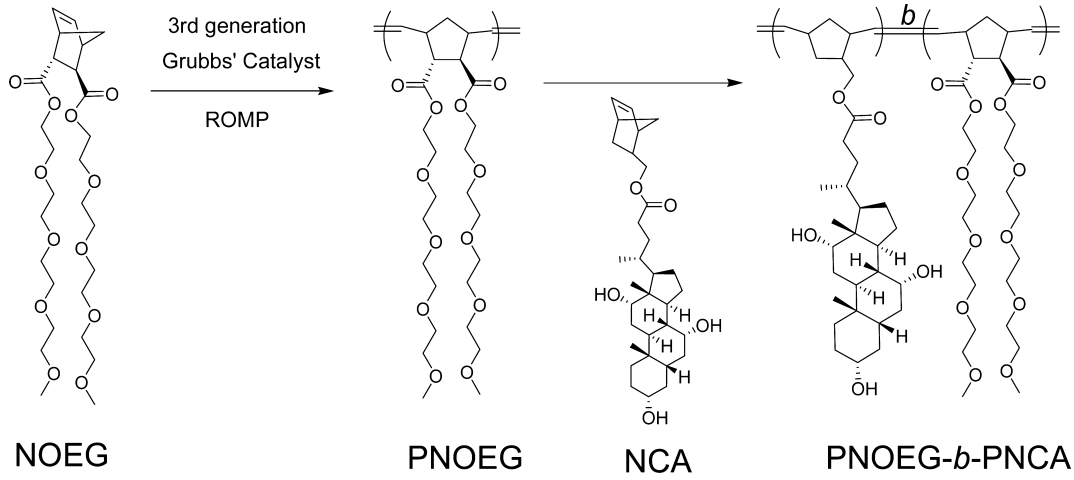

NCA was consumed. The solution was stirred for 1 h after adding ethyl vinyl ether (50 μL, 0.52 mmol). The polymer was obtained by pouring the mixture into excess cold hexane and dried *in vacuo* to yield 256 mg (98.0%) of $PNOEG_{34}$-*b*-$PNCA_8$. Here is a typical synthetic procedure of the random copolymer $P(NOEG\text{-}r\text{-}NCA)_{4:1}$. NOEG (413.5 mg, 0.735 mmol) and NCA (91.4 mg, 0.18 mmol) were dissolved in DCM (3.9 mL). Third generation Grubbs' catalyst (20.0 mg, 22.6×10^{-3} mmol) in 0.1 mL DCM was added to the monomer solution under stirring for 3 h. The solution was stirred for 1 h after adding ethyl vinyl ether (50 μL, 0.52 mmol). The polymer was obtained by pouring the mixture into excess cold hexane and dried *in vacuo* to yield 478 mg (94.8%) of random copolymer $P(NOEG\text{-}r\text{-}NCA)_{4:1}$. The other block and random copolymers with different ratios of NOEG to NCA were synthesized under similar conditions.

Preparation of PTX-Loaded Micelles. PTX was loaded into the micelles by the solvent evaporation method as described in the literature.[36] Briefly, 1 mg PTX and 10 mg of block copolymer were first dissolved in chloroform in a 10 mL round-bottom flask. The organic solvent was rotaevaporated under vacuum to form a thin film, which was further dried under high vacuum for 30 min to remove residual organic solvents. One milliliter of PBS was added to rehydrate the thin film, followed by sonication for 30 min to disperse the polymer−drug nanoconstruct into water. The loading capacity and efficiency of PTX in the micelles were determined by HPLC analysis of drug concentration of the micelle solutions before and after filtration through 0.22 μm filters. HPLC analysis used a mobile phase of 55% acetonitrile in water and a ZORBAX SB-C18 5 μm 4.6 × 150 mm column. The drug loading was calculated according to a calibration curve of the HPLC peak area versus drug concentrations.

Drug Release Study. The *in vitro* PTX release profile was studied by dialysis technique. Aliquots of the PTX-loaded micelle solution (with an initial PTX concentration of 1 g/L) were placed in a dialysis bag with a 3500 MWCO and dialyzed against 4 L water solution at room temperature with stirring at 100 rpm. The concentration of PTX remained in the dialysis cartridge at various time points was measured by HPLC and water reservoir was refreshed at the time of sampling. Values were reported as the means for each triplicate sample.

Cell Culture. SKOV-3 human ovarian adenocarcinoma cell line was purchased from American Type Culture Collection (ATCC, Manassas, VA, USA). SKOV-3 cells were cultured in McCoy's 5A Medium supplemented with 10% fetal bovine serum, 100 U/mL penicillin, and 100 mg/mL streptomycin at 37 °C using a humidified 5% CO_2 incubator.

***In Vitro* Cell Viability.** The MTS assay was used to evaluate the *in vitro* cytotoxicity of empty and PTX-loaded micelles from block and random copolymers against SKOV-3 cells. 4×10^3 cells in 95 μL culture medium were seeded in 96-well cell culture plate (Falcon) and then incubated for 24 h at 37 °C prior to the treatment. Five microliters of various formulations of PTX with different dilutions were added to each well. The cells were incubated for 72 h. MTS was added to each well and further incubated for 1−4 h. The absorbance at 490 nm was detected using a microplate ELISA reader (BioTek Synergy 2 Microplate Reader). Untreated cells served as a control. Results were shown as the average cell viability calculated from the measured optical density (OD) $[(OD_{treat} - OD_{blank})/(OD_{control} - OD_{blank}) \times 100\%]$ of triplicate wells. The cells were also treated with empty micelles with different dilutions and incubated for a total of 72 h in order to evaluate polymer-related toxicity.

RESULTS AND DISCUSSION

Synthesis of Copolymers. Block copolymers bearing cholic acid pendant groups were synthesized via ROMP of norbornene derivatives, as shown in Scheme 1, and random copolymers were also prepared by the same procedure except that both comonomers were added together (Figure S1). Generally, ROMP catalyzed by third generation Grubbs' catalyst provides control of the molecular weight, polymer composition, and distribution of pendant group along the polymer chain. Thus, the ratio of monomer to catalyst allows stoichiometric control of the molecular weight. The composition can be easily varied by changing the amounts of monomers in the feed. The molecular weights of the block and random copolymers range from 21 to 29 kDa, while their PDIs are all relatively narrow (1.10−1.25).

In general, the polymerization proceeded very fast and most of the monomers are consumed in less than 1 min. Attempts to withdraw samples at various intervals for kinetics analysis were not successful. We have shown previously that the homopolymerization of cholic acid-drivatived norbornene proceeded well with Grubbs catalyst.[33] More importantly, the final diblock had a distinctly higher molecular weight than the first block (blue vs red curves in Figure S2). There is no evidence of remaining PNOPG homopolymer in the SEC traces of the final diblock copolymer, indicating efficient chain extension of the living polymerization. This agrees well with the controlled character of the polymerization process observed by Slugovc and co-worker of norbornene-based monomers.[21] Small shoulders in the SEC traces of the copolymers (Figure S2) appeared at twice the molar mass of the primary peak. These were occasionally observed and attributed to end coupling of two polymer chains through bimolecular termination with trace amounts of oxygen.[37] These shoulders were not easily resolved from the main peak and hence were included in PDI calculations. The characteristics of these

dx.doi.org/10.1021/bm5002262 | *Biomacromolecules* 2014, 15, 1837−1844

polymers are summarized in Table 1. The use of the hydrophilic NOEG and hydrophobic NCA monomers can vary the amphiphilicity of the copolymers.

Table 1. Composition and Characteristics of the Block and Random Copolymers

polymers[a]	NOEG:NCA[b]	yield (%)	M_n[c] (g/mol)	PDI[c]	CP
$PNOEG_{34}$-*b*-$PNCA_8$	5.3:1	98.0	23 000	1.18	57.3
$PNOEG_{36}$-*b*-$PNCA_{18}$	3.4:1	96.7	29 500	1.17	52.7
$P(NOEG\text{-}r\text{-}NCA)_{4:1}$	5.0:1	94.8	28 000	1.18	56.3
$P(NOEG\text{-}r\text{-}NCA)_{3:1}$	3.1:1	95.2	25 000	1.20	53.1
PNOEG	-	92.6	16 000	1.14	68.4

[a]The subscript indicates the molar ratio of monomers in the feed. [b]Molar ratio of NOEG:NCA in copolymers calculated from ratio of ^{1}H NMR peak integrations. [c]Determined by SEC. Reaction time in all cases was 3 h.

Thermoresponsive Properties. Aqueous solutions of both $PNOEG_{34}$-*b*-$PNCA_8$ and $P(NOEG\text{-}r\text{-}NCA)_{4:1}$ show sharp phase transitions (Figure 1) with CPs at 57.3 and 56.3 °C, respectively. Their CPs seems to depend only on the molar ratios of the monomers. The phase transitions of both copolymers are reversible with a certain hysteresis (Figure 1 dashes lines). The hysteresis can be ascribed to the additional interchain hydrogen bonding formed in the collapsed state at higher temperatures, which was extensively studied by Wu and co-workers for aqueous solutions of PNIPAM.[38] The monomer ratio of NCA to NOEG has a dominant effect on the phase transition temperatures of both block and random copolymers. The CPs of these copolymer solutions (Table 1) show a decreasing trend with increasing NCA contents. The CP of $PNOEG_{34}$-*b*-$PNCA_8$ shifts to a higher temperature (58.5 °C) at a lower concentration (1.5 g/L). The phase transition becomes much broader and its CP increases further at a concentration of 1.0 g/L (Figure 1A). In contrast, the phase transition of $P(NOEG\text{-}r\text{-}NCA)_{4:1}$ is much more sensitive to concentration changes (Figure 1B). The aqueous solution of $P(NOEG\text{-}r\text{-}NCA)_{4:1}$ exhibits a phase transition over a broader temperature range (60−80 °C) at a concentration of 1.5 g/L and becomes no longer thermoresponsive when investigated at a concentration of 1.0 g/L and beyond. The broadening of the transition upon dilution, consistent with our results for other polymers,[39] is probably related to the formation of stable large aggregates rather than macroscopic phase separation when heated above the CP when the polymer concentration is between 0.1 and 1.0 g/L, as investigated by several research groups.[40−42]

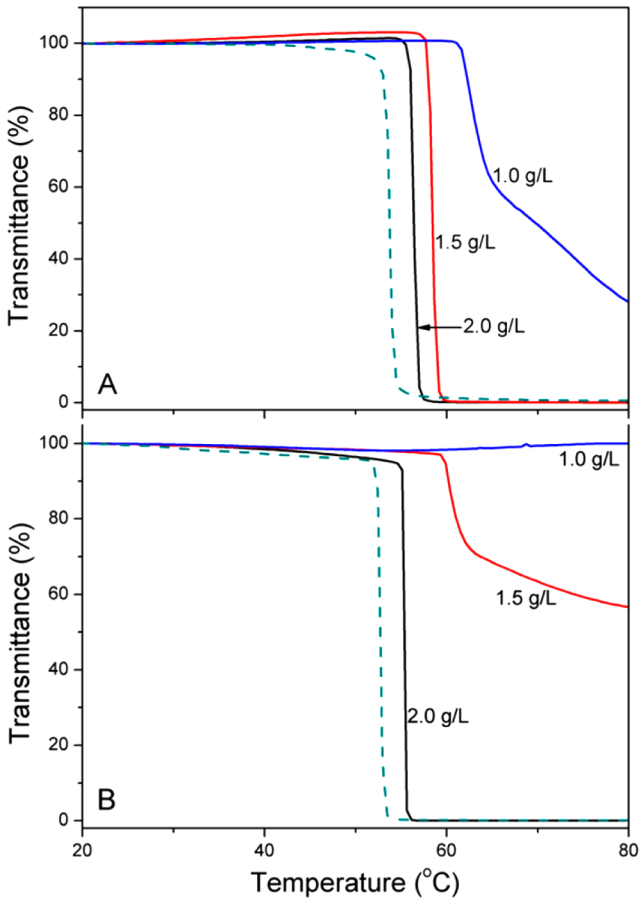

Figure 1. Variation of the transmittance of the aqueous solutions of the copolymers as a function of temperature observed at a wavelength of 400 nm and a heating (solid lines) or cooling (dashes, 2.0 g/L) rate of 0.5 °C/min. (A) $PNOEG_{34}$-*b*-$PNCA_8$ and (B) $P(NOEG\text{-}r\text{-}NCA)_{4:1}$ at the different polymer concentrations.

Self-Assembly of Block and Random Copolymers. Amphiphilic block copolymers are well-known to form nanosized micelles in aqueous milieu via intra- and/or intermolecular segregation. The CMC values of the block and random copolymers were determined by fluorescence spectroscopy with pyrene as a probe.[43] The ratio (I_{336}/I_{333}) of excitation intensities at 336 and 333 nm reflects the transition of pyrene from a polar environment to an apolar micellar core.[44,45] The excitation spectra of pyrene in solutions of copolymers show that the peak at 333 nm shifts to a longer wavelength as the copolymer concentration increases. The CMC values of $PNOEG_{34}$-*b*-$PNCA_8$ and $P(NOEG\text{-}r\text{-}NCA)_{4:1}$ are estimated to be about 5.3 mg/L and 6.0 mg/L, respectively (Table 2 and Figure S3). The block and random copolymers with similar M_n and comonomer ratios but different structural sequences show CMC values close to each other, indicating that the monomer ratio has a dominating effect on the formation of micelles. The molecular sequence in the copolymers has no significant effect on their CPs in this case, probably due in part to the relatively low molar masses of the samples.

Table 2. Micellar Properties of Block and Random Copolymers at Different Temperature in 2.0 g/L Aqueous Solutions Studied by SLS

polymer	CMC[a] (mg/L)	temperature (°C)	M_w (g/mol)	N_{agg}[b]
$PNOEG_{34}$-*b*-$PNCA_8$	5.3	25	2.09×10^6	77
		50	1.99×10^6	73
$P(NOEG\text{-}r\text{-}NCA)_{4:1}$	6.0	25	6.37×10^5	19
		50	1.35×10^6	41

[a]CMC in water measured by fluorescence with a pyrene probe at room temperature. [b]Aggregation number calculated from M_w of the micelles and of the polymers.

The intensity-average size distribution of $PNOEG_{34}$-*b*-$PNCA_8$ and $P(NOEG\text{-}r\text{-}NCA)_{4:1}$ (Figure 2A and C) indicates

dx.doi.org/10.1021/bm5002262 | Biomacromolecules 2014, 15, 1837−1844

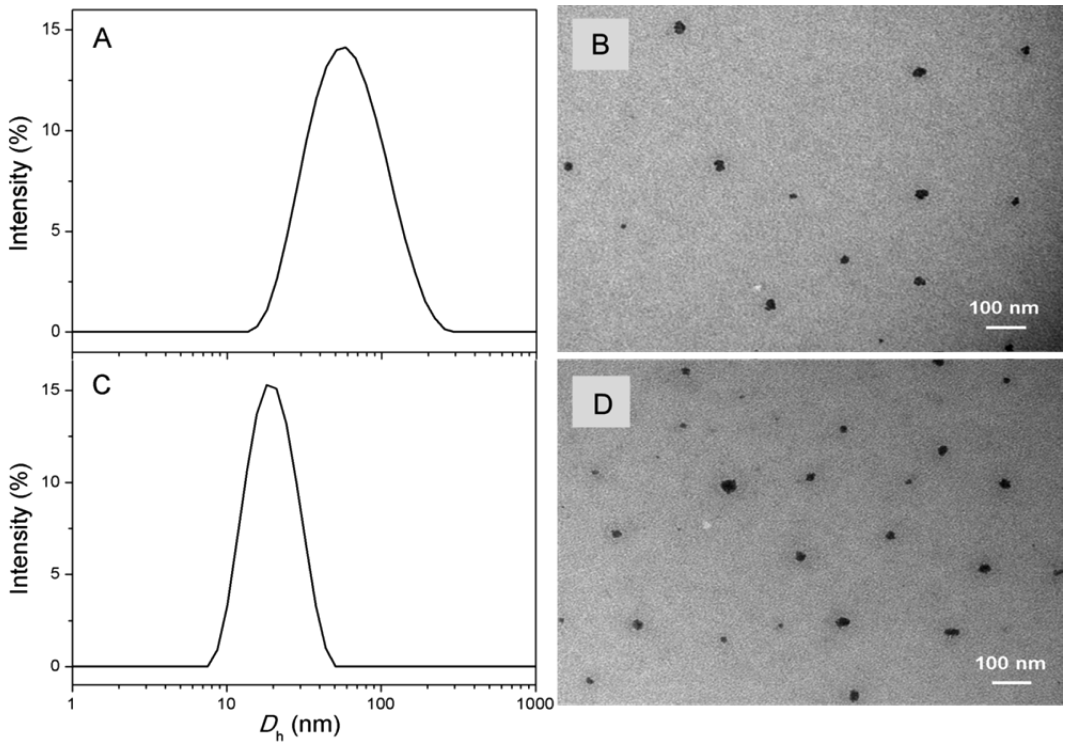

Figure 2. Intensity-average size distribution (A, C) obtained by DLS with a concentration of 2.0 g/L at 20 °C and representative TEM images (B, D, 0.2 g/L at 20 °C) of self-assembled aggregates of polymers. (A) and (B): Block copolymer $PNOEG_{34}$-*b*-$PNCA_8$. (C) and (D): Random copolymer $P(NOEG\text{-}r\text{-}NCA)_{4:1}$.

Scheme 2. Schematic Illustration of Self-Assembly and Phase Transition of Block and Random Copolymers in Water

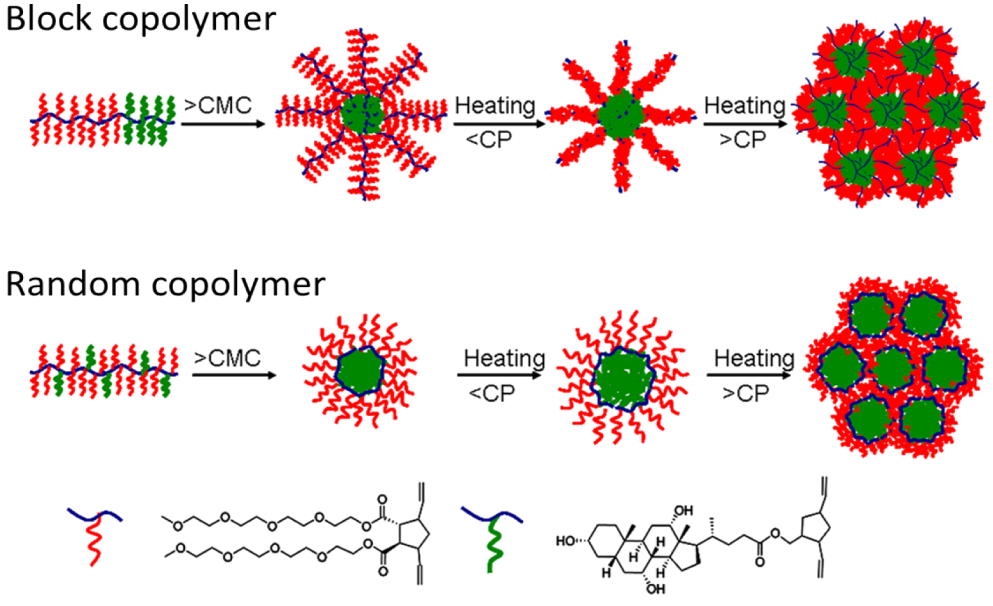

that these copolymers can both self-assemble into micelles. The average hydrodynamic diameters of the micelles formed by $PNOEG_{34}$-*b*-$PNCA_8$ and by $P(NOEG\text{-}r\text{-}NCA)_{4:1}$ are around 65 and 20 nm, respectively. Both show unimodal distributions. The smaller size of the polymeric micelles formed by random copolymers is interesting and intriguing; to the best of our knowledge, the comparison of the micelles formed by random and block copolymers of similar composition remains a subject not yet much studied. The difference in micellar size may result from the different self-assembled core−shell structures of the block and random copolymers. The hydrophilic PNOEG block forms the shell of the micelles of the block copolymer, whereas only short PEG side chains self-assemble into the shell in the case of the random copolymer (Scheme 2). Therefore, the shell of the micelles formed by the block copolymer may be much thicker than that of the random copolymer, leading to the larger apparent size of the micelles formed by the block copolymer. Note that the aggregation numbers for the micelles of the block copolymer are also larger (Table 2).

dx.doi.org/10.1021/bm5002262 | *Biomacromolecules* 2014, 15, 1837−1844

The formation of micelles by both the block and random copolymers with a hydrophobic cholic acid core surrounded by a hydrophilic PEG shell leads to the disappearance of the ^{1}H NMR signals from the core components (Figure S4B).[46] The signals of the methylene of PEG chains (3.3−3.7 ppm) and methyl group of cholic acid (0.6−1.1 ppm) were clearly observed in $CDCl_3$. For example, the peaks of $PNOEG_{34}$-*b*-$PNCA_8$ in $CDCl_3$ at 0.70, 0.90, and 1.01 ppm were assigned to methyl protons of cholic acid at positions 18, 19, and 21, respectively (Figure S4A). The peak at 3.40 ppm was associated with the methoxyl protons on PEG chains. When the $CDCl_3$ was replaced by D_2O in the ^{1}H NMR experiment, no signal of the methyl proton on cholic acid was observed (Figure S4B), indicating that the core−shell micellar structures of the block copolymer in water. In contrast, for the D_2O solution of the random copolymer, weak signals of methyl groups on cholic acid moieties were observed (Figure S4C), indicating a greater mobility of the cholic acid-containing segments in this case.

TEM images (Figure 2B and D) show that both $PNOEG_{34}$-*b*-$PNCA_8$ and P(NOEG-*r*-NCA)$_{4:1}$ self-assemble into micelles and are well dispersed as individual nanoparticles with a regular shape. However, the diameter of micelles formed by $PNOEG_{34}$-*b*-$PNCA_8$ (ca. 30 nm in Figure 2B) is slightly smaller than that measured by DLS, whereas the diameter of some micelles formed by P(NOEG-*r*-NCA)$_{4:1}$ (ca. 35 nm in Figure 2D) is somewhat larger than that measured by DLS. This may be interpreted in terms of different core−shell structures of the block and random copolymers. In the case of the block copolymer, the thick hydrophilic shell is sufficient to stabilize the core of the micelles in solution. These micelles shrank during the drying process,[47] so that the diameter measured by TEM is slightly smaller than that measured by DLS. With regard to the micelles formed by the random copolymer P(NOEG-*r*-NCA)$_{4:1}$, the relatively thin PEG shell (Scheme 2) may not be sufficient to stabilize the core of the isolated micelles. SLS results revealed the weight-average mass (M_w) of the micelles formed by P(NOEG-*r*-NCA)$_{4:1}$ increased from ca. 6.37×10^5 to 1.35×10^6 as the temperature rose from 25 to 50 °C (Table 2 and Figure S5), effectively doubling the aggregation number (N_{agg}) of the micellar aggregates. In comparison, the N_{agg} of the micelles formed by $PNOEG_{34}$-*b*-$PNCA_8$ remained unchanged with rising temperature since its M_w changed from ca. 2.09 to 1.99×10^6 in the same temperature range. Note that micellar clusters may also form during the drying process, as the TEM images also show heterogeneity of the size of the aggregates.

The CPs of $PNOEG_{34}$-*b*-$PNCA_8$ and P(NOEG-*r*-NCA)$_{4:1}$ did not exhibit any significant difference as shown by the temperature-dependent DLS results (Figure 3A). However, the hydrodynamic diameters (D_h) of the micelles formed by the block and random copolymers (Figure 3A) showed different temperature-dependent behaviors below their CPs. The D_h of the micelles formed by $PNOEG_{34}$-*b*-$PNCA_8$ gradually decreased from 65 to 30 nm when the temperature was raised from 20 to 54 °C. In contrast, the micelles formed by P(NOEG-*r*-NCA)$_{4:1}$ showed a small increase in size from 20 to 26 nm in the same temperature range. These behaviors may be related to the different self-assembled core−shell structures of the block and random copolymers. The thick hydrophilic shell of micelles formed by $PNOEG_{34}$-*b*-$PNCA_8$ may shrink below its CP due to the reorganization of the interdigitated PEG chains, which is consistent with the results reported previously.[48,49] The micelles formed by the random copolymer

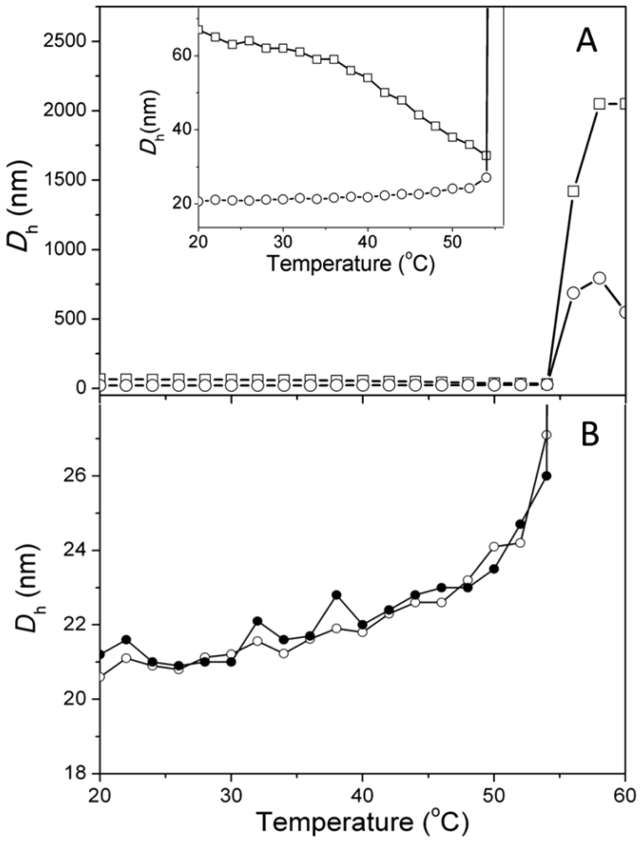

Figure 3. Hydrodynamic diameter of polymer aggregates in aqueous solutions as a function of temperature (2.0 g/L): (A) $PNOEG_{34}$-*b*-$PNCA_8$ (squares) and P(NOEG-*r*-NCA)$_{4:1}$ (circles) under heating; (B) P(NOEG-*r*-NCA)$_{4:1}$ under heating (opened circles) and cooling (solid circles) cycles.

are more dynamic in solution, probably facilitated by the thinner hydrophilic shell. The SLS results confirmed that the micellar aggregation number (N_{agg}) of the micelles formed by the random copolymer increases with rising temperature,[50] leading to the swelling of the micelles, while those formed by the block copolymer remains more stable in the same temperature range (Table 2). Interestingly, the swelling of the micelles formed by P(NOEG-*r*-NCA)$_{4:1}$ was almost perfectly reversible during cooling cycles as shown in Figure 3B, whereas the shrinkage of the micelles formed by $PNOEG_{34}$-*b*-$PNCA_8$ below CP is not reversible during cooling (Figure S6).

Based on these results, a mechanism is proposed for the thermally induced phase transition of these copolymers. In Scheme 2, the aggregation process is illustrated and the relative changes in size and aggregation number are also shown schematically. First, both the block and random copolymers in water self-assemble into well-defined micelles above their CMCs. When the temperature is below their CPs, the micelles formed by the block copolymers showed a broad and gradual shrinkage, whereas a slightly gradual swelling was observed for the micelles formed by the random copolymers. When the micellar solution is heated to the phase transition temperature, the dehydration of the PEG corona caused by the disruption of hydrogen bonds between the polymer and water leads to the formation of larger aggregates of the micelles for both the block and random copolymers.

Loading and Release of PTX. PTX was loaded into micelles at a polymer concentration of 10.0 g/L and a theoretical drug loading content (DLC) of 10.0 wt %. The micelles formed by $PNOEG_{34}$-*b*-$PNCA_8$ and P(NOEG-*r*-NCA)$_{4:1}$ exhibited PTX loading efficiencies of 79.1% and 88.8%, respectively (Table 3). Contrary to conventional thinking, after drug loading into the micellar core, the hydrodynamic diameter of resulting micelles actually showed a significant decrease in size. This is intriguing but not unusual, and may be attributed to the tightening of the micelles caused by the enhanced hydrophobic interaction between the drug and the micelle core.[51] *In vitro* drug release studies were carried out at room temperature with a dialysis tube (MWCO 3500) in water. As shown in Figure 4A, 78% and 24% of PTX were released at the point of 24 h in the cases of $PNOEG_{34}$-*b*-$PNCA_8$ and P(NOEG-*r*-NCA)$_{4:1}$, respectively. The release of PTX from the random copolymer-formed micelles was significantly slower than from the block copolymer micelles at room temperature. This result is quite interesting and even somewhat unusual, and may be attributable to the more densely assembled micellar structure of the random copolymer P(NOEG-*r*-NCA)$_{4:1}$ at relatively low temperatures, as illustrated in Scheme 2.

Table 3. Physicochemical Properties of $PNOEG_{34}$-*b*-$PNCA_8$ and P(NOEG-*r*-NCA)$_{4:1}$

polymers[a]	CMC[a] (mg/L)	micellar size[b] (nm)	PTX loading efficiency[c] (%)	micellar size with PTX[d] (nm)
$PNOEG_{34}$-*b*-$PNCA_8$	5.3	65	79.1 ± 2.6	24
P(NOEG-*r*-NCA)$_{4:1}$	6.0	20	88.8 ± 4.0	17

[a]Determined in water by fluorescence with a pyrene probe at room temperature. [b]Size of empty micelles formed by block and random copolymers. [c]PTX loading efficiency of the micelles, in the presence of 10 g/L of block and random copolymers, measured by HPLC. [d]PTX loading of micelles was 1 g/L, respectively.

The antitumor activity of PTX-loaded micelles (Figure 4B) was investigated in SKOV-3 cell with MTS assay. The cells were incubated with PTX-loaded micelles or free PTX for 72 h. The results showed that the PTX-loaded micelles formed by $PNOEG_{34}$-*b*-$PNCA_8$ and P(NOEG-*r*-NCA)$_{4:1}$ induced pronounced antitumor effects to the ovarian cancer cells. The viability of SKOV-3 cells was reduced to about 40% following 72 h incubation with 100 ng PTX equiv/mL PTX-loaded micelles. Notably, PTX-loaded micelles displayed similar efficacy with the free PTX formulation in SKOV-3 cell. The maximal half-inhibitory concentrations (IC_{50}) were determined to be 27.4, 40.2, and 44.5 ng of PTX equiv/mL for the drug-loaded micelles formed by the block and random copolymers, respectively. The higher antitumor activity of PTX-loaded micelles of the block copolymer in comparison to the random copolymer might be due to their faster drug release in cell culture, which is in good agreement with *in vitro* drug release results. The empty micelles formed by the block and random copolymers were practically nontoxic (cell viability ~100%) up to a tested concentration of 1.0 g/L, supporting that micelles based on cholic acid-based polymers possess good biocompatibility. With the slower and almost linear drug release profile and the similar anticancer effect (Figure 4), the PTX-loaded micelles formed by the random copolymer may be more appropriate for *in vivo* anticancer treatments, since less drug leakage into the blood circulation for the slower release profile may reduce the adverse effects of drug toxicity and deliver more drug content to tumor site via the enhanced permeability and retention effects.

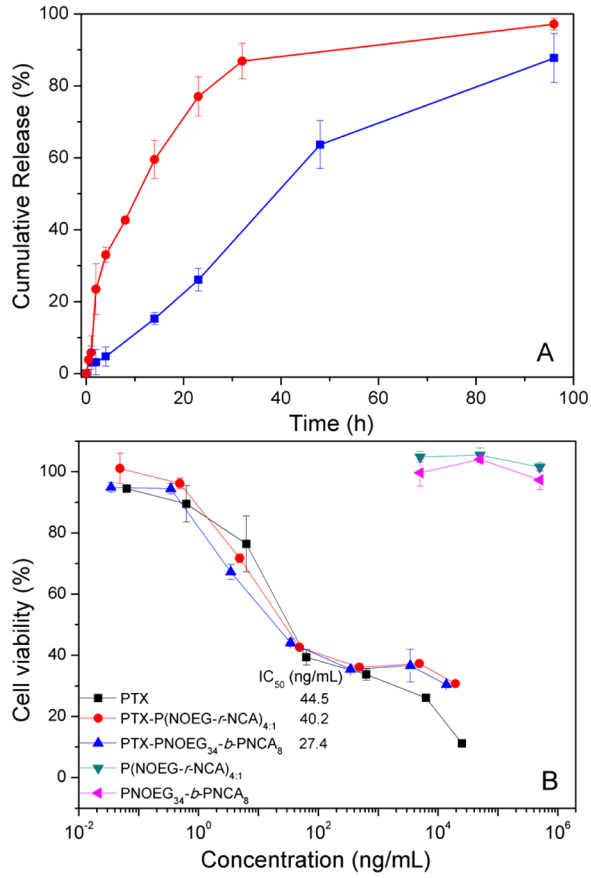

Figure 4. (A) *In vitro* PTX release profiles from the micelles formed by the block copolymer $PNOEG_{34}$-*b*-$PNCA_8$ (circles) and the random copolymer P(NOEG-*r*-NCA)$_{4:1}$ (squares) via dialysis against water at room temperature (PTX: 1 g/L and polymer: 10 g/L). (B) Cytotoxicity of empty micelles and cancer cell killing activity of the free PTX (in 50% of Cremophor EL in dry ethanol) and PTX-loaded micelles formed by the block and random copolymers as a function of PTX concentration. All data are presented as the average ± standard deviation (n = 3).

CONCLUSION

Both block and random copolymers containing cholic acid and PEG pendent groups were synthesized via ROMP. These copolymers are amphiphilic in nature and exhibited responsive properties toward temperature. The phase transition temperature of the copolymers could be tuned by variation of the monomers ratios. DLS and TEM results revealed both the block and random copolymers self-assembled into micelles in water. Below their CPs, the dynamic nature of the micelles formed by the random copolymer caused an increased N_{agg} with rising temperature leading to a gradual swelling while the micelles of the block copolymer exhibited a gradual shrinkage in the same temperature range. Through *in vitro* drug release experiments and MTT assay, we have demonstrated that micelles formed by the block and random copolymers can actively load a hydrophobic anticancer drug PTX and can also efficiently deliver and release PTX into tumor cells, achieving high antitumor activity comparable to that of free PTX. The micelles from cholic acid-based polymer are highly promising

dx.doi.org/10.1021/bm5002262 | *Biomacromolecules* 2014, 15, 1837−1844

for the delivery of hydrophobic anticancer drugs. The random copolymer may be better suited for the drug release application due to the close to linear release profiles. The *in vivo* tumor targeting and anticancer effects of these two formulations will be further evaluated.

■ ASSOCIATED CONTENT

Supporting Information

The synthetic scheme of the norbornene monomer NCA and NOEG as well as the random copolymer, SEC traces of the block copolymer $PNOEG_{34}$-*b*-$PNCA_8$, CMC determination, and ^1H NMR spectra of the $PNOEG_{34}$-*b*-$PNCA_8$ and $P(NOEG\text{-}r\text{-}NCA)_{4:1}$, as well as hydrodynamic diameter of $PNOEG_{34}$-*b*-$PNCA_8$ under heating and cooling cycle. This material is available free of charge via the Internet at http://pubs.acs.org.

■ AUTHOR INFORMATION

Corresponding Author

*E-mail: julian.zhu@umontreal.ca.

Notes

The authors declare no competing financial interest.

■ ACKNOWLEDGMENTS

Financial support from NSERC of Canada, FQRNT of Quebec, and the Canada Research Chair program is gratefully acknowledged. The authors of U de M are members of CSACS funded by FQRNT and GRSTB funded by FRSQ. C.Y. Shi and J.T. Luo are supported by NIH/NCI R01CA140449 and Carol M. Baldwin Breast Cancer Research Foundation. We thank Dr. S. Strandman for her help with the TEM, Ms N. Xue for her help with the SLS measurements.

■ REFERENCES

(1) Zhang, C. Y.; Yang, Y. Q.; Huang, T. X.; Zhao, B.; Guo, X. D.; Wang, J. F.; Zhang, L. J. *Biomaterials* **2012**, *33*, 6273−6283.
(2) Endres, T. K.; Beck-Broichsitter, M.; Samsonova, O.; Renette, T.; Kissel, T. H. *Biomaterials* **2011**, *32*, 7721−7731.
(3) Li, G.; Liu, J.; Pang, Y.; Wang, R.; Mao, L.; Yan, D.; Zhu, X.; Sun, J. *Biomacromolecules* **2011**, *12*, 2016−2026.
(4) Webster, O. W. *Science* **1991**, *251*, 887−893.
(5) Choi, T.-L.; Grubbs, R. H. *Angew. Chem.* **2003**, *115*, 1785−1788.
(6) Leitgeb, A.; Wappel, J.; Slugovc, C. *Polymer* **2010**, *51*, 2927−2946.
(7) Bielawski, C. W.; Grubbs, R. H. *Prog. Polym. Sci.* **2007**, *32*, 1−29.
(8) Wang, F.; Bronich, T. K.; Kabanov, A. V.; Rauh, R. D.; Roovers, J. *Bioconjugate Chem.* **2005**, *16*, 397−405.
(9) Arotçaréna, M.; Heise, B.; Ishaya, S.; Laschewsky, A. *J. Am. Chem. Soc.* **2002**, *124*, 3787−3793.
(10) Soppimath, K. S.; Tan, D. C. W.; Yang, Y. Y. *Adv. Mater.* **2005**, *17*, 318−323.
(11) Patrickios, C. S.; Hertler, W. R.; Abbott, N. L.; Hatton, T. A. *Macromolecules* **1994**, *27*, 930−937.
(12) Chung, J. E.; Yokoyama, M.; Yamato, M.; Aoyagi, T.; Sakurai, Y.; Okano, T. *J. Controlled Release* **1999**, *62*, 115−127.
(13) Liu, R.; Fraylich, M.; Saunders, B. *Colloid Polym. Sci.* **2009**, *287*, 627−643.
(14) Wei, H.; Zhang, X.-Z.; Zhou, Y.; Cheng, S.-X.; Zhuo, R.-X. *Biomaterials* **2006**, *27*, 2028−2034.
(15) Zhou, Q.; Zhang, Z.; Chen, T.; Guo, X.; Zhou, S. *Colloids Surf., B* **2011**, *86*, 45−57.
(16) Talelli, M.; Hennink, W. E. *Nanomedicine* **2011**, *6*, 1245−1255.
(17) Zarafshani, Z.; Obata, T.; Lutz, J.-F. *Biomacromolecules* **2010**, *11*, 2130−2135.
(18) Lutz, J.-F. *J. Polym. Sci.: Polym. Chem.* **2008**, *46*, 3459−3470.
(19) Lutz, J.-F.; Hoth, A. *Macromolecules* **2006**, *39*, 893−896.
(20) Zarafshani, Z.; Obata, T.; Lutz, J.-F. *Biomacromolecules* **2010**, *11*, 2130−2135.
(21) Bauer, T.; Slugovc, C. *J. Polym. Sci.: Polym. Chem.* **2010**, *48*, 2098−2108.
(22) Mukhopadhyay, S.; Maitra, U. *Curr. Sci.* **2004**, *87*, 1666−1684.
(23) Hofmann, A.; Hagey, L. *Cell. Mol. Life Sci.* **2008**, *65*, 2461−2483.
(24) Xiao, K.; Luo, J.; Fowler, W. L.; Li, Y.; Lee, J. S.; Xing, L.; Cheng, R. H.; Wang, L.; Lam, K. S. *Biomaterials* **2009**, *30*, 6006−6016.
(25) Li, Y.; Xiao, W.; Xiao, K.; Berti, L.; Luo, J.; Tseng, H. P.; Fung, G.; Lam, K. S. *Angew. Chem., Int. Ed.* **2012**, *51*, 2864−2869.
(26) Zhang, Y. H.; Zhu, X. X. *Macromol. Chem. Phys.* **1996**, *197*, 3473−3482.
(27) Hao, J.; Li, H.; Zhu, X. X. *Biomacromolecules* **2006**, *7*, 995−998.
(28) Li, C.; Lavigueur, C.; Zhu, X. X. *Langmuir* **2011**, *27*, 11174−11179.
(29) Liu, H.; Avoce, D.; Song, Z.; Zhu, X. X. *Macromol. Rapid Commun.* **2001**, *22*, 675−680.
(30) Avoce, D.; Liu, H. Y.; Zhu, X. X. *Polymer* **2003**, *44*, 1081−1087.
(31) Love, J. A.; Morgan, J. P.; Trnka, T. M.; Grubbs, R. H. *Angew. Chem., Int. Ed.* **2002**, *41*, 4035−4037.
(32) Zhang, G.; Wu, C. *Adv. Polym. Sci.* **2006**, *195*, 101−176.
(33) Shao, Y.; Lavigueur, C.; Zhu, X. X. *Macromolecules* **2012**, *45*, 1924−1930.
(34) Pulamagatta, B.; Pankaj, S.; Beiner, M.; Binder, W. H. *Macromolecules* **2011**, *44*, 958−965.
(35) Sandholzer, M.; Fritz-Popovski, G.; Slugovc, C. *J. Polym. Sci.: Polym. Chem.* **2008**, *46*, 401−413.
(36) Luo, J.; Xiao, K.; Li, Y.; Lee, J. S.; Shi, L.; Tan, Y.-H.; Xing, L.; Holland Cheng, R.; Liu, G.-Y.; Lam, K. S. *Bioconjugate Chem.* **2010**, *21*, 1216−1224.
(37) Perrott, M. G.; Novak, B. M. *Macromolecules* **1995**, *28*, 3492−3494.
(38) Cheng, H.; Shen, L.; Wu, C. *Macromolecules* **2006**, *39*, 2325−2329.
(39) Jia, Y.; Zhu, X. X.; Liu, L.; Li, J. *Langmuir* **2012**, *28*, 4500−4506.
(40) Cai, W. S.; Gan, L. H.; Tam, K. C. *Colloid Polym. Sci.* **2001**, *279*, 793−799.
(41) Verbrugghe, S.; Laukkanen, A.; Aseyev, V.; Tenhu, H.; Winnik, F. M.; Du Prez, F. E. *Polymer* **2003**, *44*, 6807−6814.
(42) Gorelov, A. V.; Du Chesne, A.; Dawson, K. A. *Physica A* **1997**, *240*, 443−452.
(43) Chen, Y.; Luo, J.; Zhu, X. X. *J. Phys. Chem. B* **2008**, *112*, 3402−3409.
(44) Bae, J. W.; Lee, E.; Park, K. M.; Park, K. D. *Macromolecules* **2009**, *42*, 3437−3442.
(45) Morinaga, H.; Morikawa, H.; Wang, Y.; Sudo, A.; Endo, T. *Macromolecules* **2009**, *42*, 2229−2235.
(46) Kang, Y.; Taton, T. A. *J. Am. Chem. Soc.* **2003**, *125*, 5650−5651.
(47) Khlebtsov, N. G. *Colloid J.* **2003**, *65*, 652−655.
(48) Zhulina, E. B.; Borisov, O. V.; Pryamitsyn, V. A.; Birshtein, T. M. *Macromolecules* **1991**, *24*, 140−149.
(49) Zhang, W.; Zhou, X.; Li, H.; Fang, Y.; Zhang, G. *Macromolecules* **2005**, *38*, 909−914.
(50) Messaoud, T.; Duplatre, G.; Michels, B.; Waton, G. *J. Phys. Chem. B* **2004**, *108*, 13137−13143.
(51) Zhang, L.; Zhao, C.; Zhou, J.; Kondo, T. *J. Mater. Chem. C* **2013**, *1*, 5756−5764.